Glacier flow and sliding


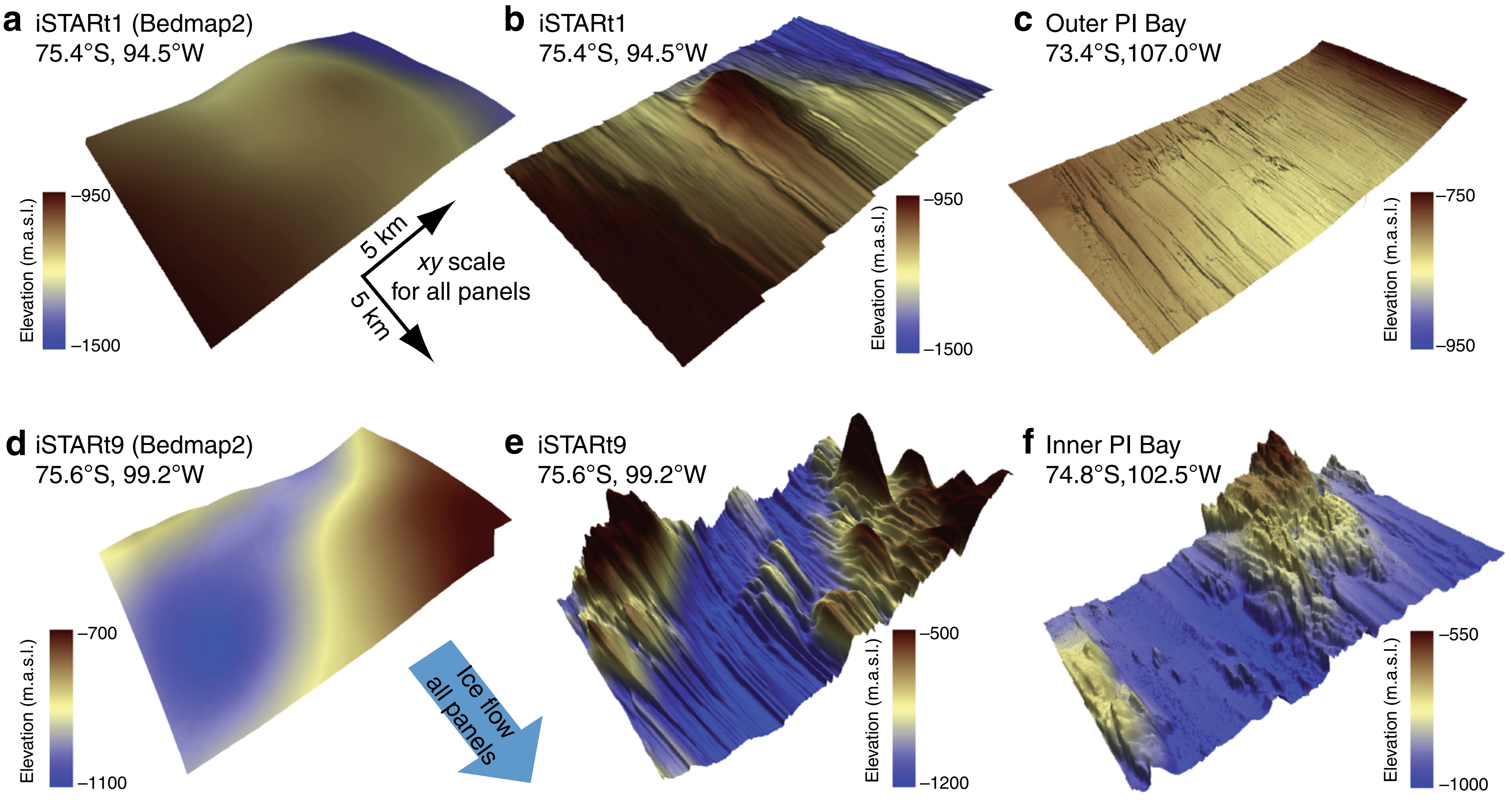

Bingham et al 2017, Kyrke-Smith et al 2018

Inversion of basal friction in Antarctica using exact and incomplete adjoints of a higher-order model

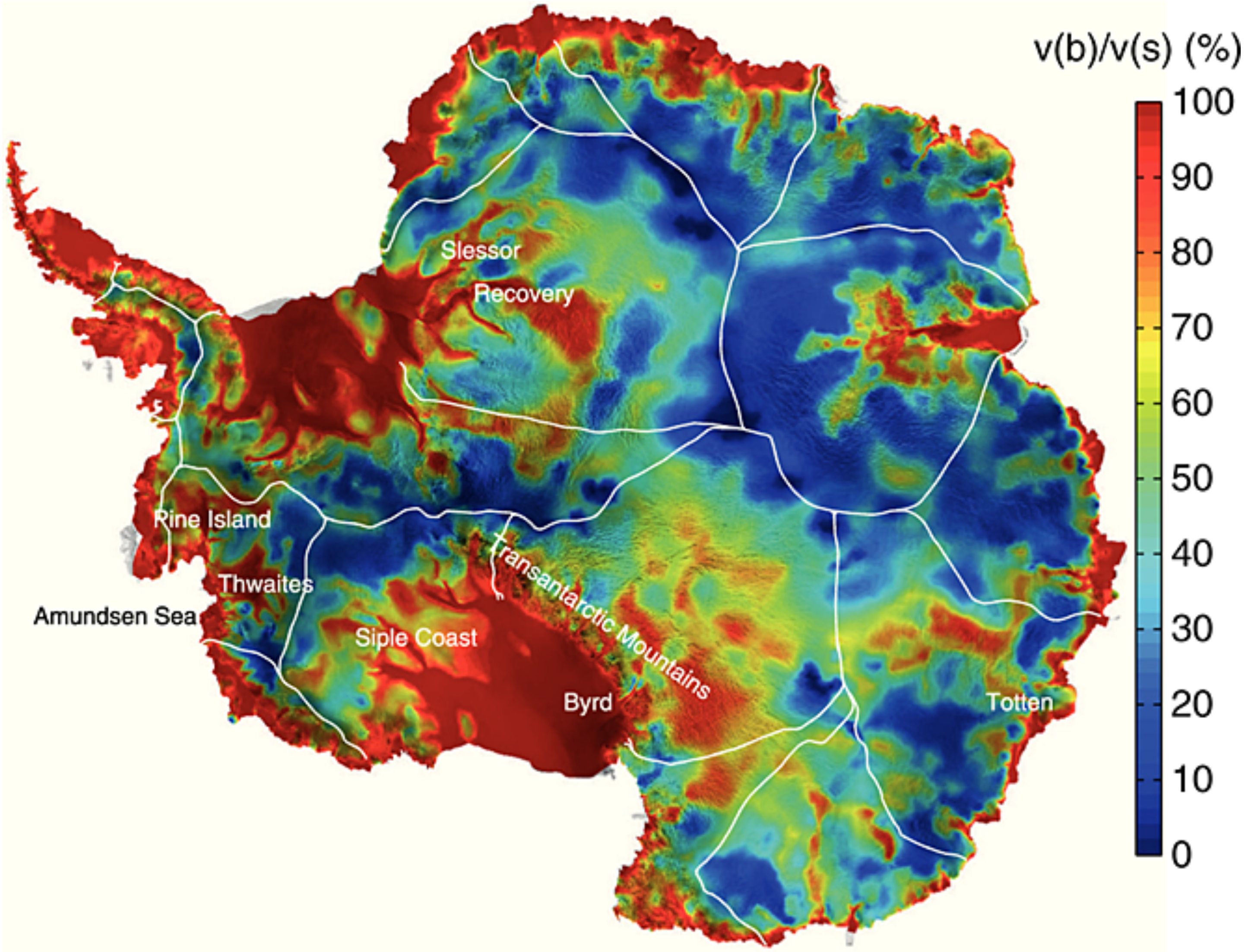

Inversion of basal friction in Antarctica using exact and incomplete adjoints of a higher-order model, Volume: 118, Issue: 3, Pages: 1746-1753, First published: 30 July 2013, DOI: (10.1002/jgrf.20125)

Glacier Flow

Surface time lapse: https://youtu.be/1ai9Q27J2vc

Bed time lapse: https://youtu.be/njTjfJcAsBg

Glacier flow

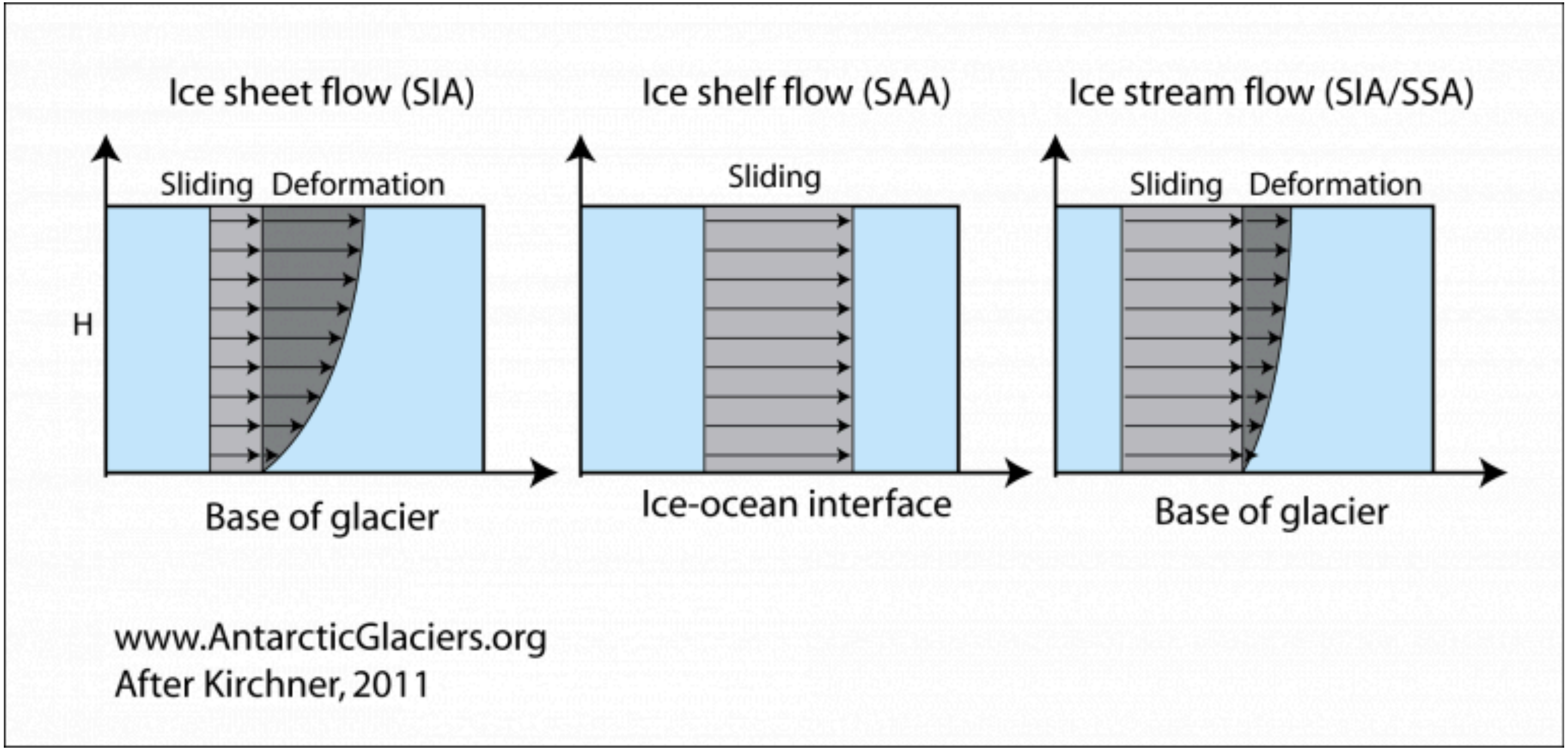

Glacier Flow

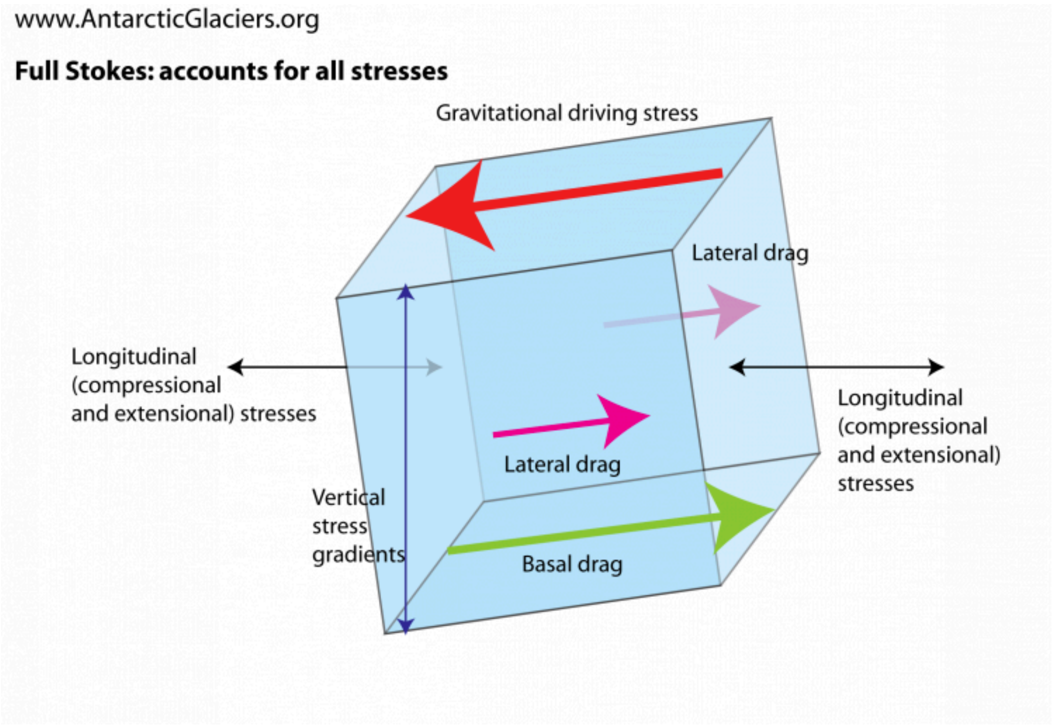

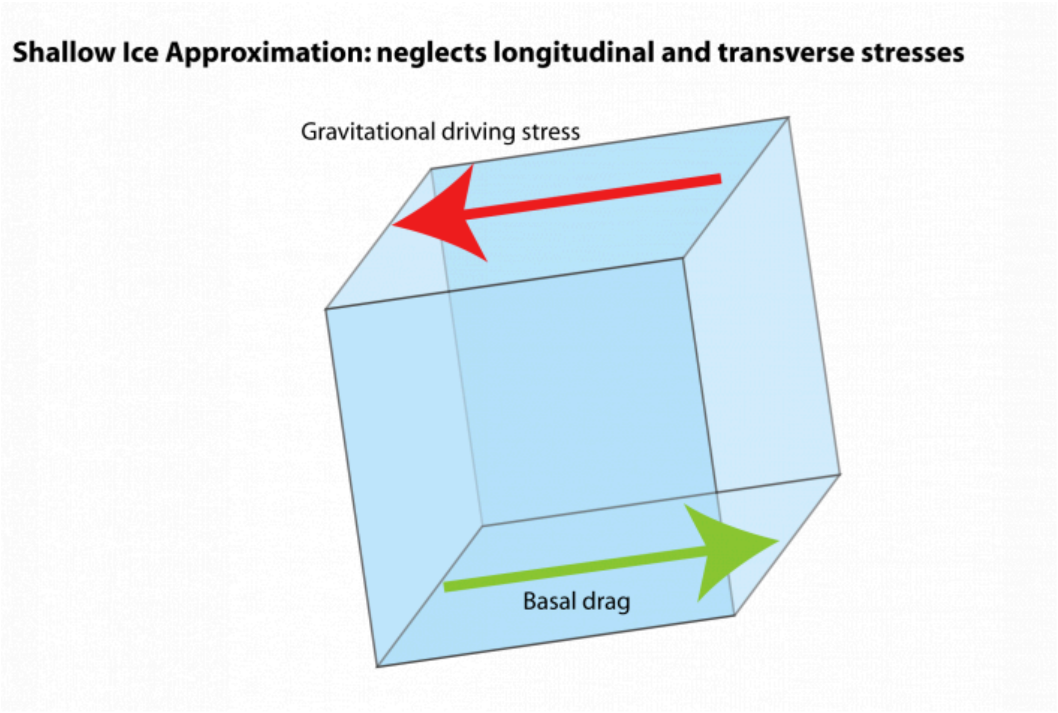

Glacier flow

$$\begin{cases} \frac{\partial}{\partial x}\left(2\mu\frac{\partial v_x}{\partial x}\right) + \frac{\partial}{\partial y}\left(\mu\frac{\partial v_x}{\partial y} + \mu\frac{\partial v_y}{\partial x}\right) + \frac{\partial}{\partial z}\left(\mu\frac{\partial v_x}{\partial z} + \mu\frac{\partial v_z}{\partial x}\right) - \frac{\partial p}{\partial x} = 0 \\ \frac{\partial}{\partial x}\left(\mu\frac{\partial v_x}{\partial y} + \mu\frac{\partial v_y}{\partial x}\right) + \frac{\partial}{\partial y}\left(2\mu\frac{\partial v_y}{\partial y}\right) + \frac{\partial}{\partial z}\left(\mu\frac{\partial v_y}{\partial z} + \mu\frac{\partial v_z}{\partial y}\right) - \frac{\partial p}{\partial y} = 0 \\ \frac{\partial}{\partial x}\left(\mu\frac{\partial v_x}{\partial z} + \mu\frac{\partial v_z}{\partial x}\right) + \frac{\partial}{\partial y}\left(\mu\frac{\partial v_y}{\partial z} + \mu\frac{\partial v_z}{\partial y}\right) + \frac{\partial}{\partial z}\left(2\mu\frac{\partial v_z}{\partial z}\right) - \frac{\partial p}{\partial z} - \rho g = 0 \end{cases}$$

$$\frac{\partial v_x}{\partial x} + \frac{\partial v_y}{\partial y} + \frac{\partial v_z}{\partial z} = 0$$

Glacier flow: strain rate components

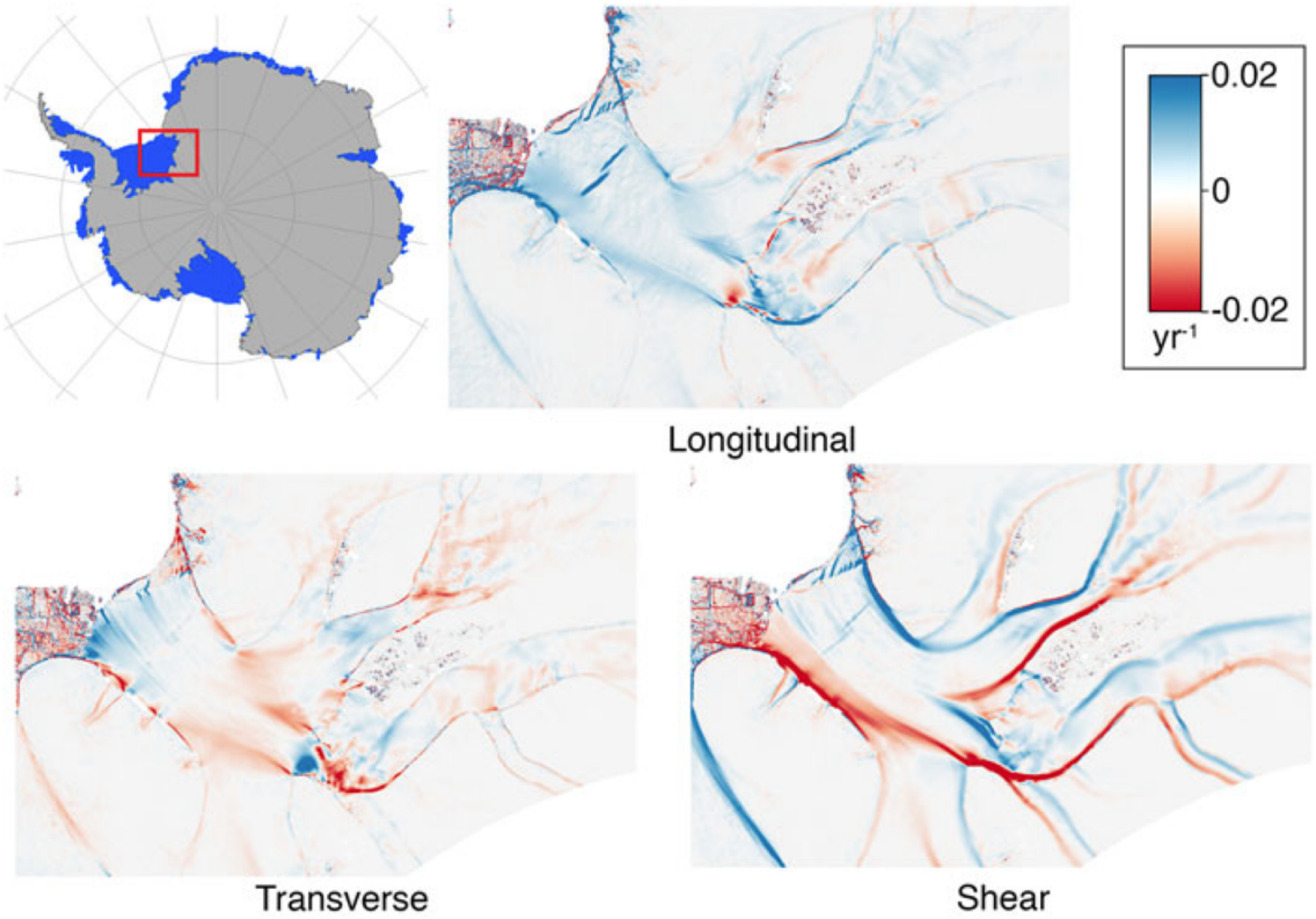

Alley et al., 2018

Ice viscosity

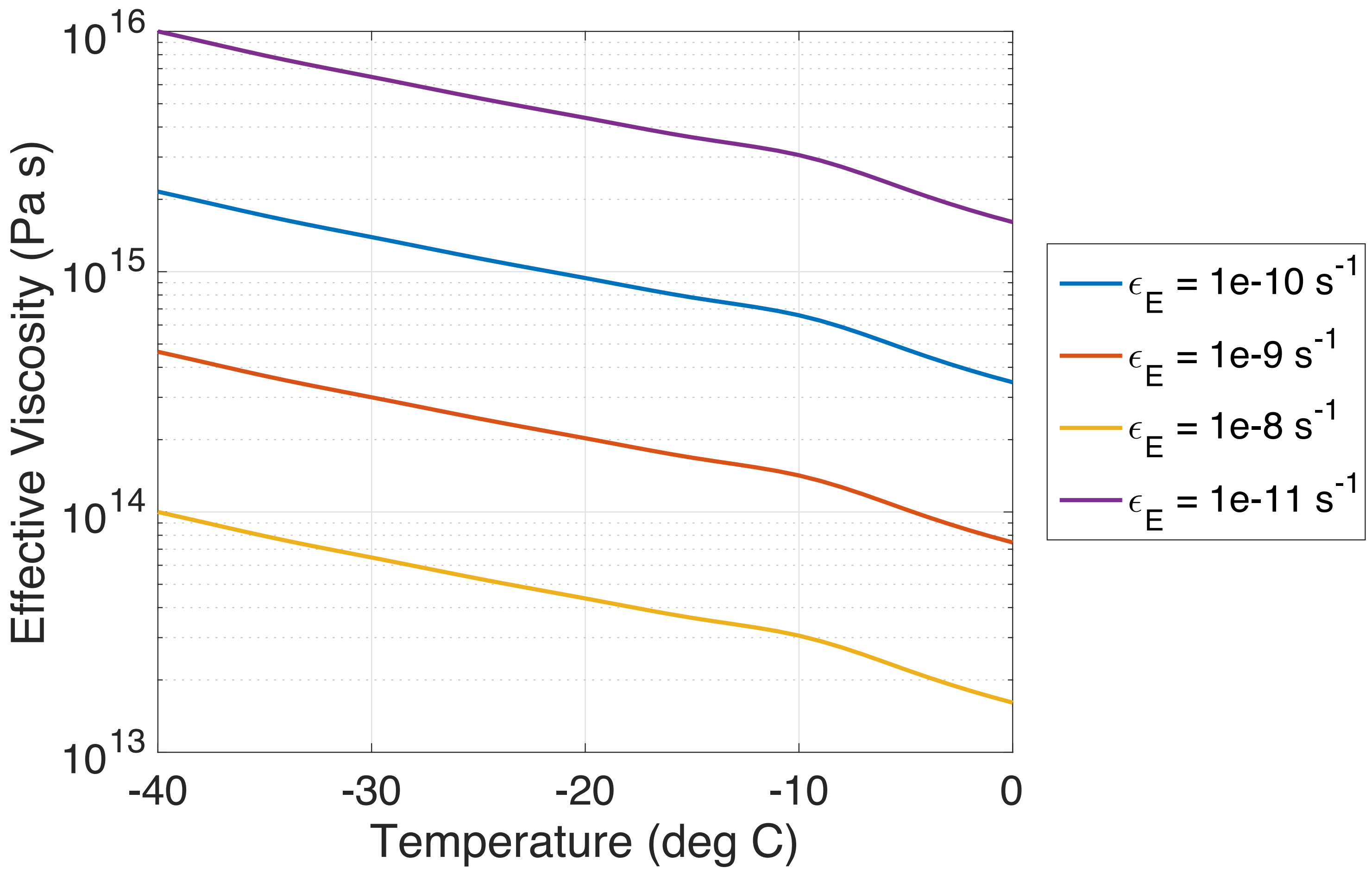

Coupling different flow regimes

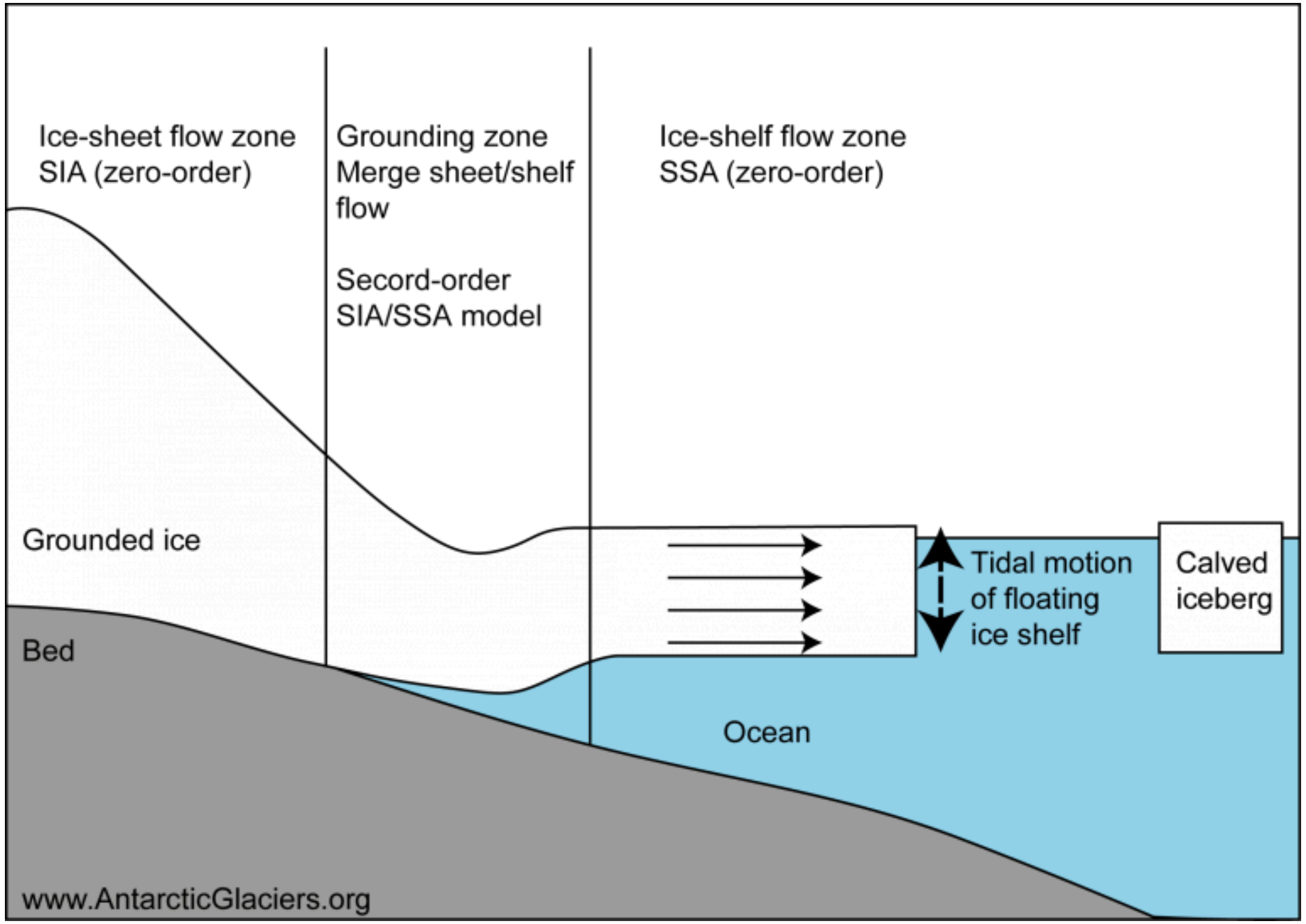

Sliding Laws

- The “Correct” sliding law for a particular application requires knowledge of the processes at play.
- These are fundamentally *parameterizations,* meaning that they are simplified representations of unresolved processes.

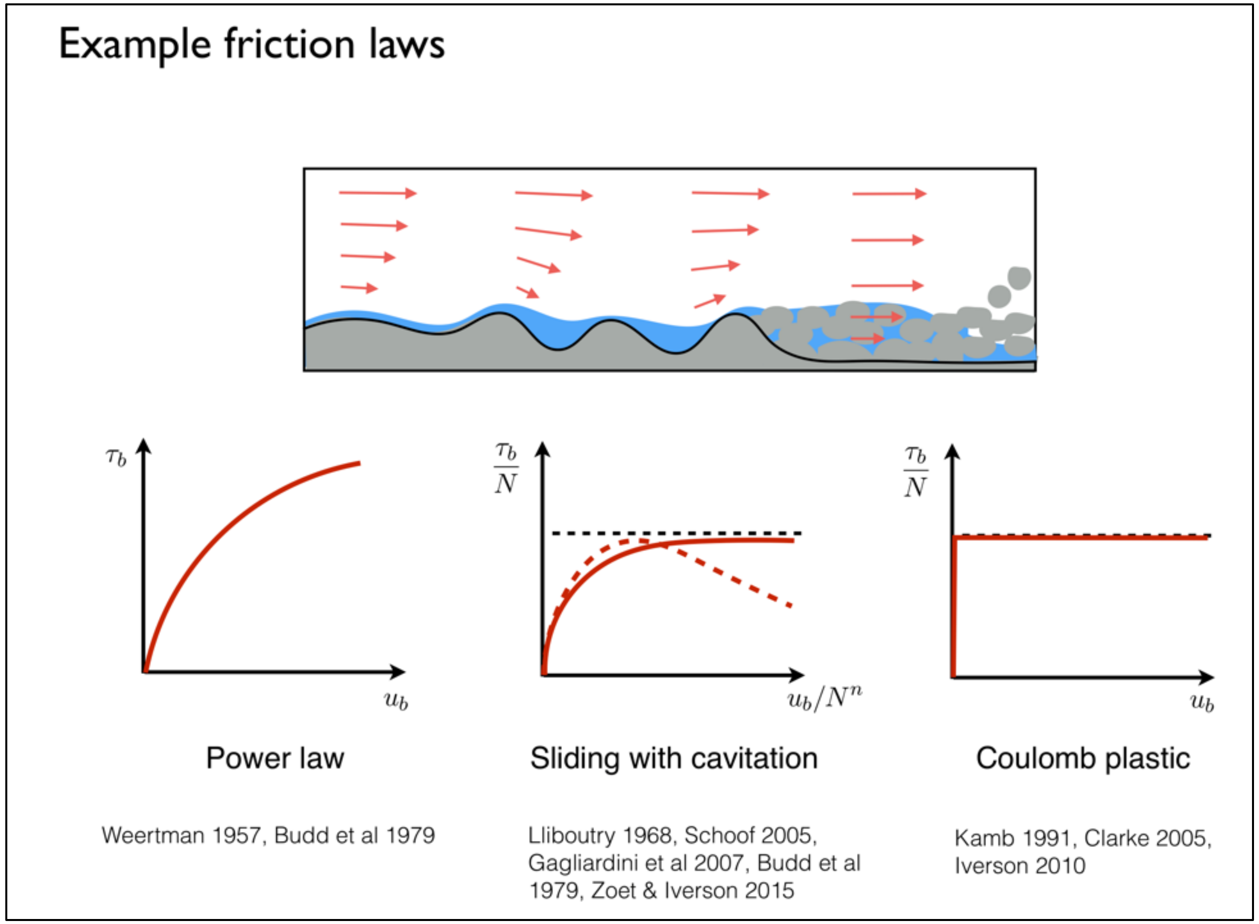

Slides from Ian Hewitt’s presentation at the Karthaus Summer School.

Hard-bedded sliding Weertman 1957

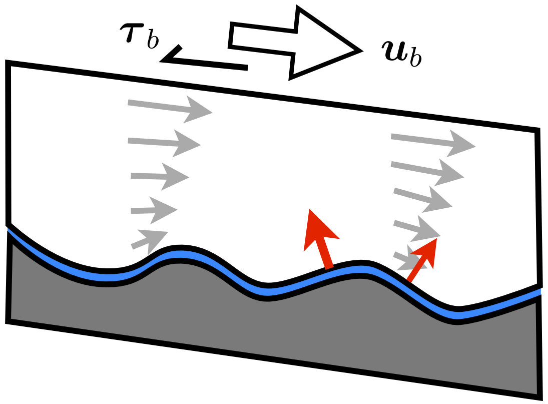

A **film of water** exists between ice and the underlying bedrock (a few microns thick).

Microscopically, free slip is allowed (i.e. $\tau_{b \text{ micro}} = 0$).

Macroscopic resistance comes from the **roughness** of the bedrock ($\tau_{b \text{ macro}} = f(U_b)$).

Flow over roughness occurs via **regelation** and **viscous (plastic) deformation**.

Slides from Ian Hewitt's presentation at the Karthaus Summer School.

Regelation

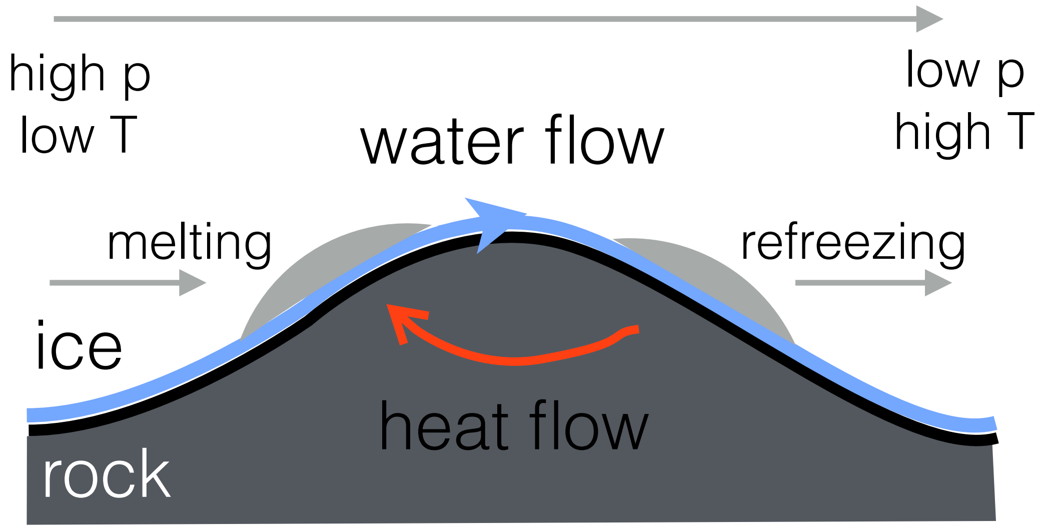

Viscous flow

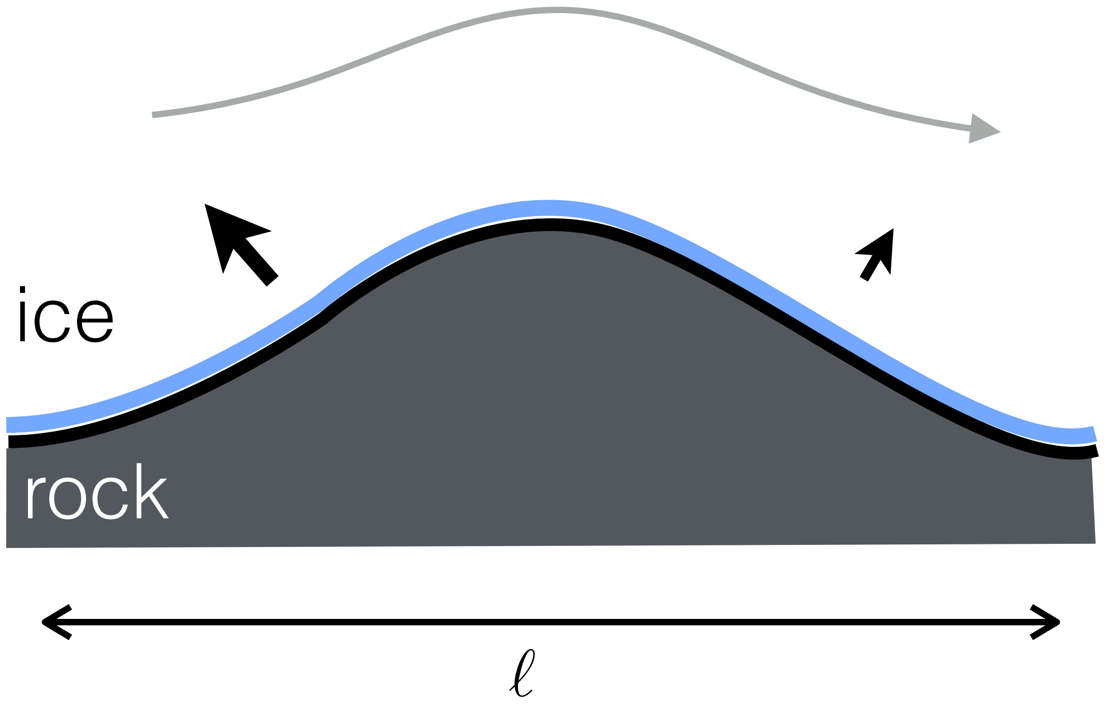

Slides from Ian Hewitt's presentation at the Karthaus Summer School.

Nye-Kamb theory Nye 1969, Kamb 1970

A more sophisticated approach to (Newtonian) viscous flow and regelation

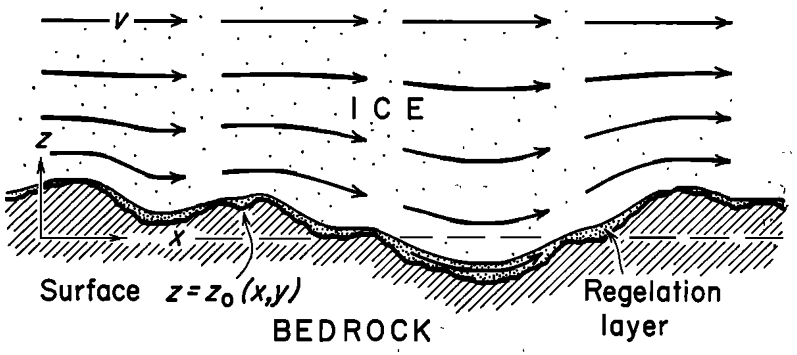

Kamb 1970

Stokes flow $\nabla^4\psi = 0$

Heat equation $\nabla^2 T = 0$

via Fourier transform
$$\boxed{\tau_b = \eta_i U_b \frac{k_*^2}{\pi}\int_0^\infty \frac{\hat{Z}_b(k)k^3}{k^2+k_*^2}\mathrm{d}k}$$

effective ice viscosity $\eta_i \sim 1/A\tau_b^{n-1}$

transitional wavenumber $k_* = \left(\frac{\rho_i L}{4k\Gamma\eta_i}\right)^{1/2} \sim 2\pi/50\ \mathrm{cm}$

regelation important
for short wavelengths

power spectrum of bed profile $\hat{Z}_b(k) = \lim_{M\to\infty}\frac{1}{M}\left|\int_{-M}^{M} Z_b(x)e^{ikx}\,\mathrm{d}x\right|$

Slides from Ian Hewitt's presentation at the Karthaus Summer School.

Viscous flow and regelation

Combining these two mechanisms:

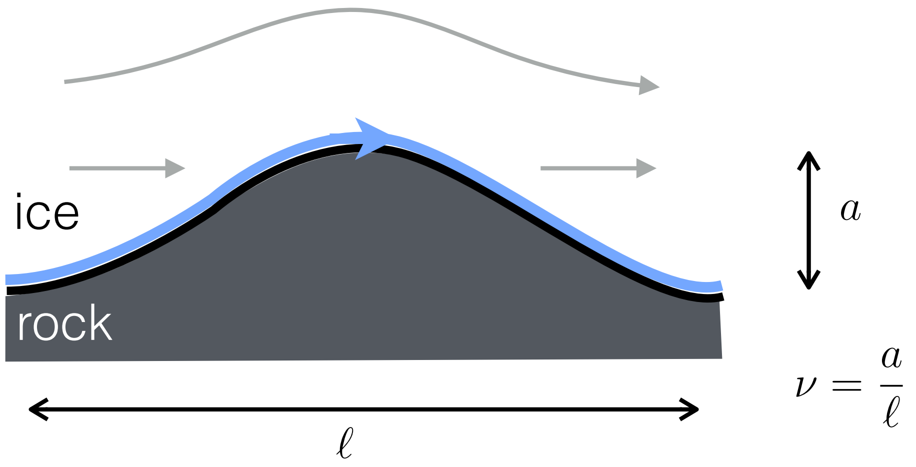

$$U_V \approx \left(\frac{aA}{2^n}\right)\frac{\tau_b^n}{\nu^{2n}}$$ effective for LARGE bumps

$$U_R = \left(\frac{k\Gamma}{\rho_i L a}\right)\frac{\tau_b}{\nu^2}$$ effective for SMALL bumps

There is a '**controlling obstacle size**' for which stress / speed cross over: $a \propto U_b^{-(n-1)/(n+1)}$

⇨ Weertman sliding law $\boxed{\tau_b = \nu^2 \; R \; U_b^{2/(n+1)}}$

$$R = \left(\frac{\rho_i L}{2k\Gamma A}\right)^{1/(n+1)}$$

Slides from Ian Hewitt's presentation at the Karthaus Summer School.

Sliding with cavitation Lliboutry 1968

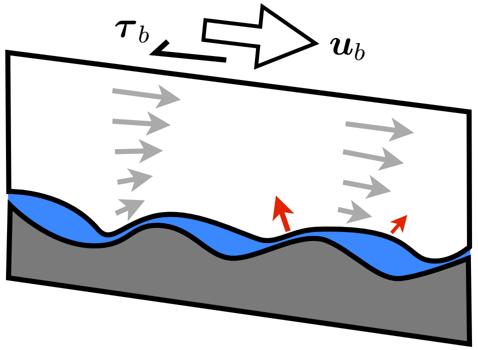

Cavitation occurs when pressure on downstream face of bumps reduces to critical level p_c

Sliding law becomes dependent on **effective pressure** $N = p_i - p_c$

p_i (macroscopic) ice normal stress

$\Rightarrow$ $\boxed{\tau_b = f(U_b, N)}$

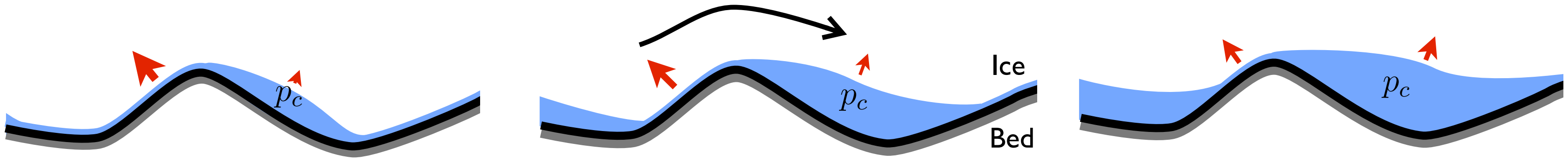

Decreased p_c
High N

Increased p_c
Low N

Slides from Ian Hewitt's presentation at the Karthaus Summer School.

Cavitation Experiments (Zoet and Iverson 2015, 2016)

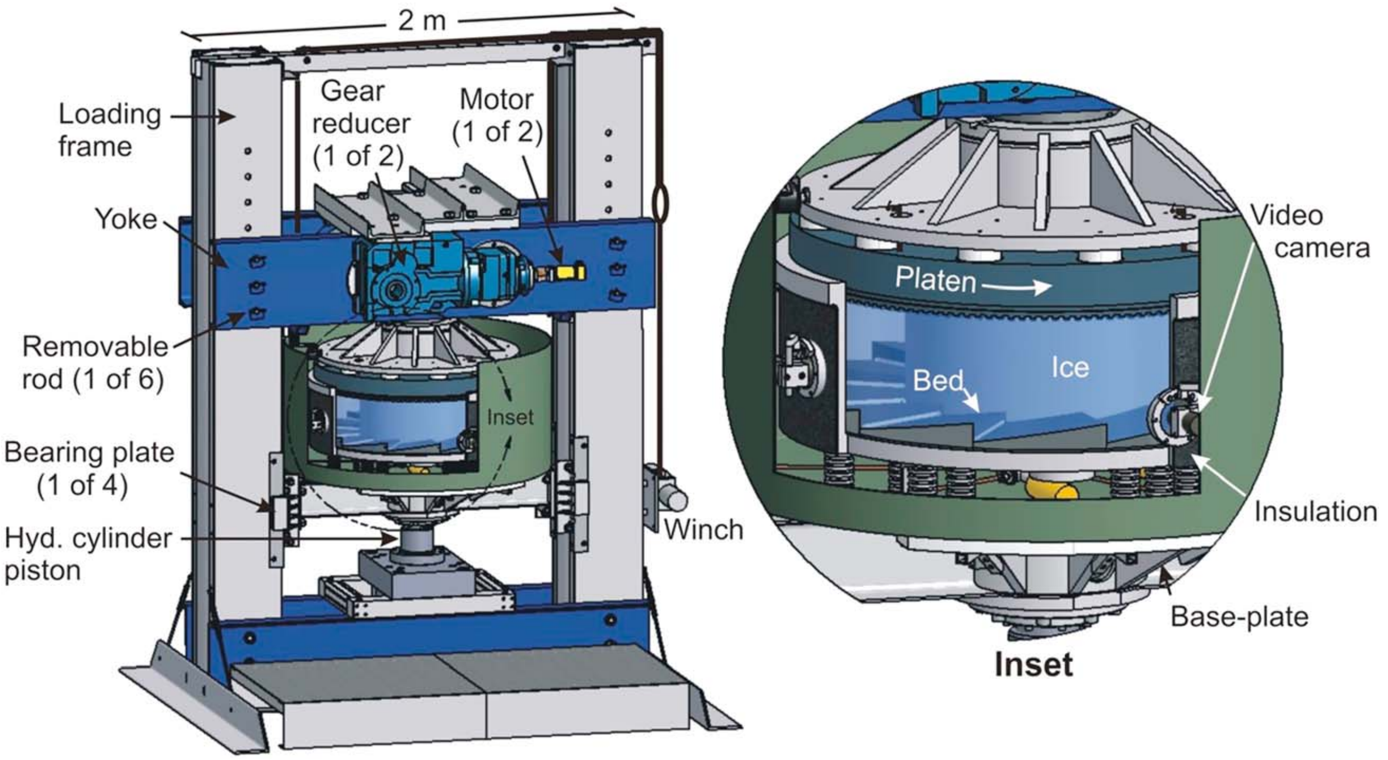

Figure 2. Device schematic used for sliding experiments. The inset details the sample chamber containing the stepped bed. An annular plate with teeth grips the ice ring at its upper surface and drags it across the bed and along smooth walls that confine the ice ring laterally.

Cavitation Experiments (Zoet and Iverson 2015, 2016)

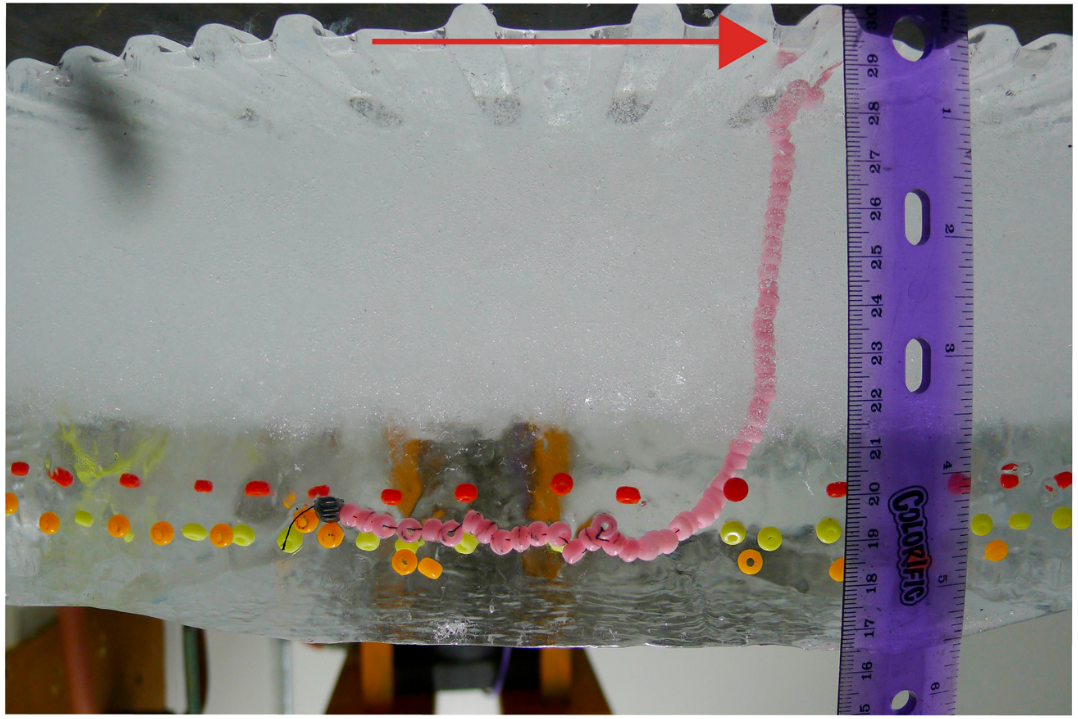

Figure 7. Ice deformation. Along-flow view of the ice ring at the end of an experiment, showing displacement of beads (pink) that were in a vertical column prior to sliding. The upper surface was gripped and displaced to the right (as denoted by the arrow) as ice slid across the bed. Note that left side of the scale is in centimeters. Nonpink beads were used to track sliding displacement and were not initially in vertical columns. Clear ice in the lowermost 40% of the ice ring reflects recrystallization during ice deformation that purged air bubbles from the ice.

Cavitation Experiments (Zoet and Iverson 2015, 2016)

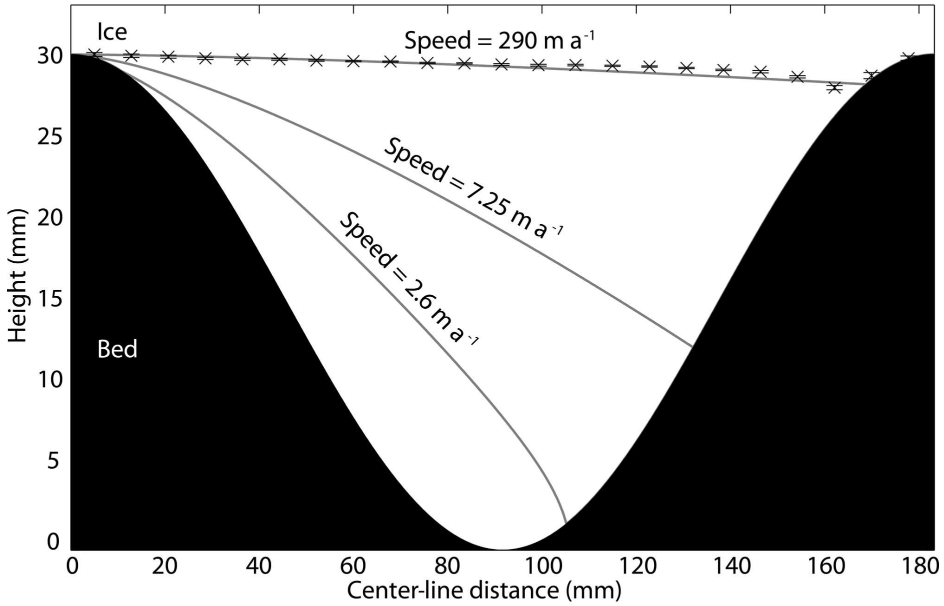

Fig. 3. Cavities at the bed due to sliding. Longitudinal profiles of cavities at the ice-ring center line at sliding speeds of 2.6, 7.25 and 290 m a^{-1} (gray lines), under a total vertical stress of 500 kPa and atmospheric pressure in cavities. Cavity geometry at 290 m a^{-1} was both measured directly (crosses) and fitted (gray line) using the theory of Kamb (1987), as described in the Appendix. Error bars indicate $\pm 1\sigma$ of variability based on measurements of multiple cavities. Note the exaggerated vertical scale.

Cavitation Experiments (Zoet and Iverson 2015, 2016)

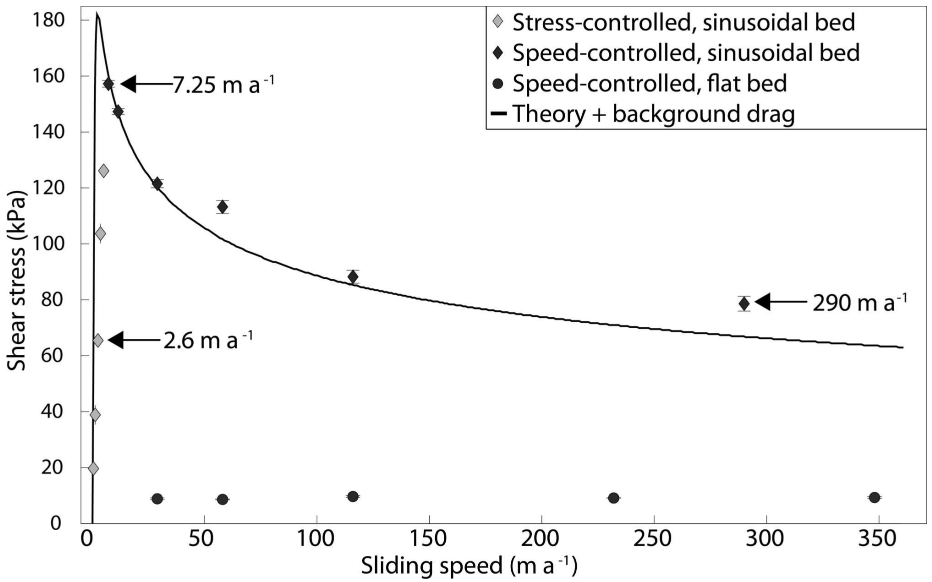

Fig. 4. Drag on the bed. Mean steady shear stress as a function of sliding speed for a sinusoidal bed and a flat bed. Error bars indicate $\pm 1\sigma$ from the mean, once a time-averaged steady stress or speed was reached (e.g. Fig. 2). The speeds (2.6, 7.25 and 290 m a^{-1}) correspond to the cavity geometries of Figure 3. The solid line is the sum of the shear stress estimated using a theory of sliding in the presence of cavities (Lliboutry, 1968, 1979) and the background shear stress measured with the flat bed.

Sliding with cavitation

Lliboutry 1968, Iken 1981,1983

Lliboutry suggested the sliding relationship was **non-monotonic** - a 'multivalued' sliding law

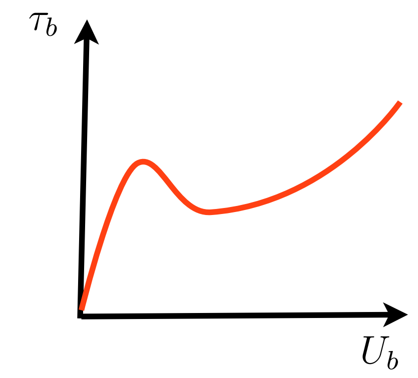

Iken suggested there should be a **maximum shear stress**

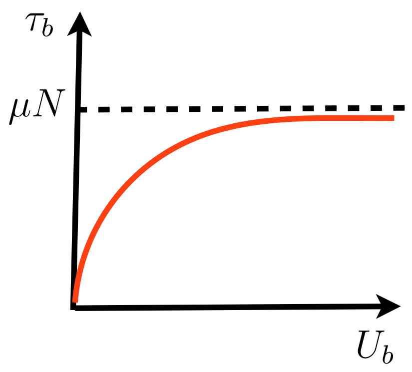

associated with cavities 'drowning' the bed roughness.

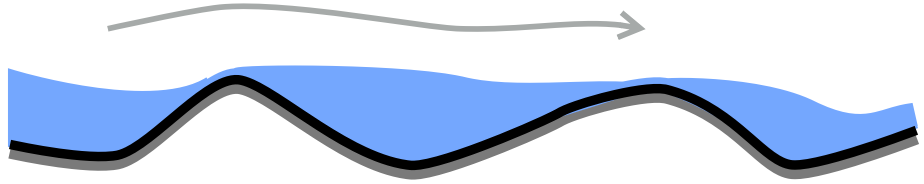

Slides from Ian Hewitt's presentation at the Karthaus Summer School.

Sliding with cavitation

Fowler 1986, Schoof 2005, Gagliardini et al 2007

Fowler suggests cavities never really 'drown' bed - stress is just transferred to larger bumps

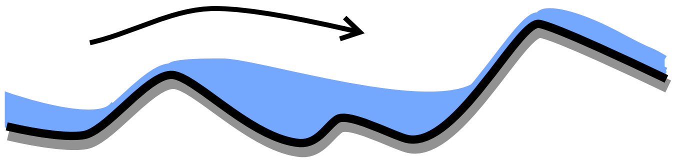

⇨ $\tau_b = N f\left(\frac{U_b}{N^n}\right)$

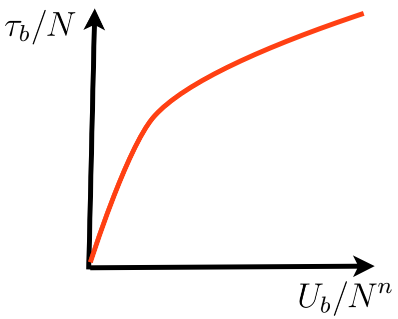

⇨ 'Generalized' Weertman law $\boxed{\tau_b = C U_b^p N^q}$ $0 < p, q < 1$

Some experimental support for this law with $p = q = \frac{1}{3}$ (Budd et al 1979)

Schoof suggests an alternative with a maximum shear stress

⇨ Regularised 'Coulomb' law $\boxed{\frac{\tau_b}{N} = \mu\left(\frac{U_b}{U_b + \lambda A N^n}\right)^{1/n}}$

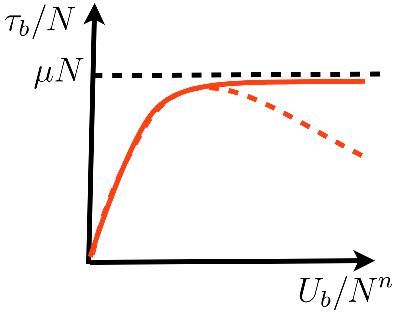

Slides from Ian Hewitt's presentation at the Karthaus Summer School.

Soft-bedded sliding

Boulton & Hindmarsh 1987, Kamb 1991, Tulaczyk 2000, Clarke 2005

Subglacial till has a complicated rheology (more complicated than ice)

Laboratory experiments suggest **plastic** behaviour, i.e. no deformation beneath a yield stress

$$\tau_f = \cancel{c_0} + \sigma_e \tan\psi$$

$$\sigma_e = P - p_w \approx N$$ effective stress

$$\tan\psi \approx 0.44$$

When yield stress exceeded, there are two main possibilities:

- Visco-plastic model $\dot{\varepsilon} = A(\tau - \tau_f)^a \sigma_e^b$

  Till layer depth h_T $\boxed{U_b = h_T A \tau_b^a N^b}$

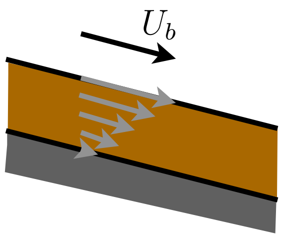

- Perfect plasticity $\tau = \tau_f$ $\boxed{\tau_b = \mu N}$

  Stress must be transferred laterally to sticky spots

  No 'local' sliding law in this case

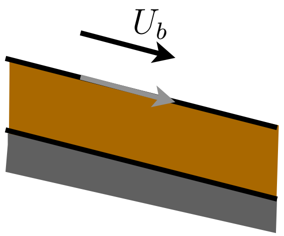

Slides from Ian Hewitt's presentation at the Karthaus Summer School.

Summary

Hard bedrock

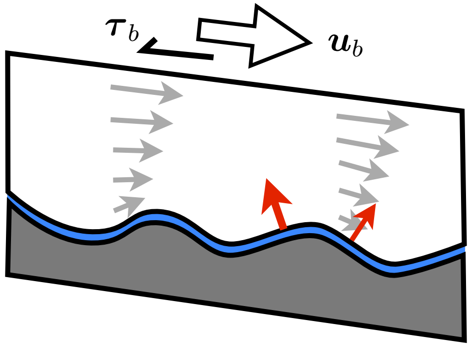

$$\tau_b = R U_b^{1/m}$$

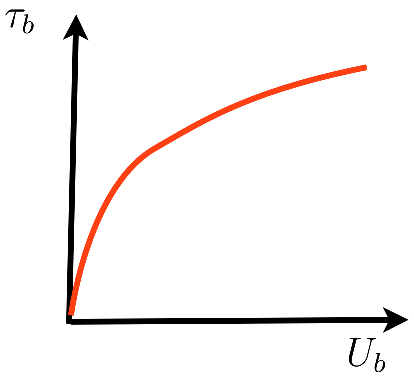

Cavities

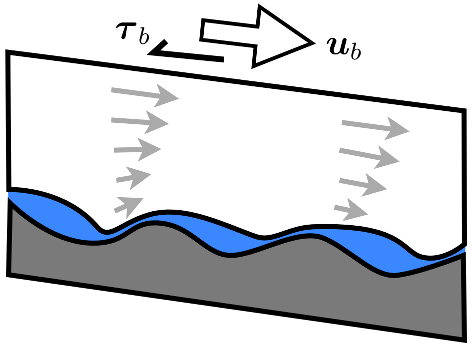

$$\tau_b = C U_b^p N^q$$

$$\tau_b = \mu N \left(\frac{U_b}{U_b + \lambda A N^n} \right)^{1/n}$$

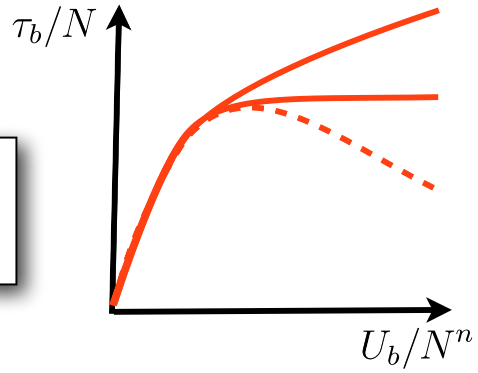

Soft sediments

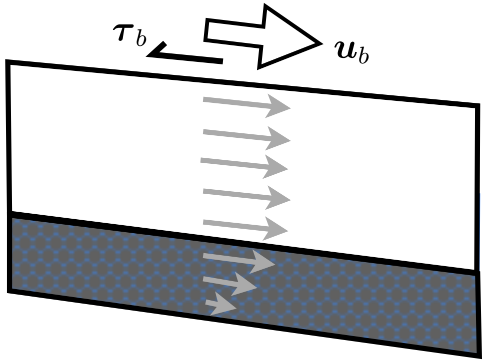

$$\tau_b = \mu N$$

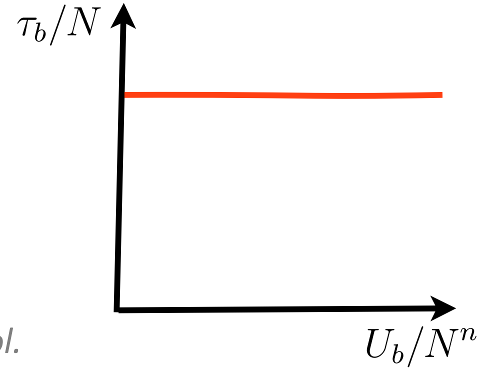

Slides from Ian Hewitt's presentation at the Karthaus Summer School.

Sliding on fine grained beds

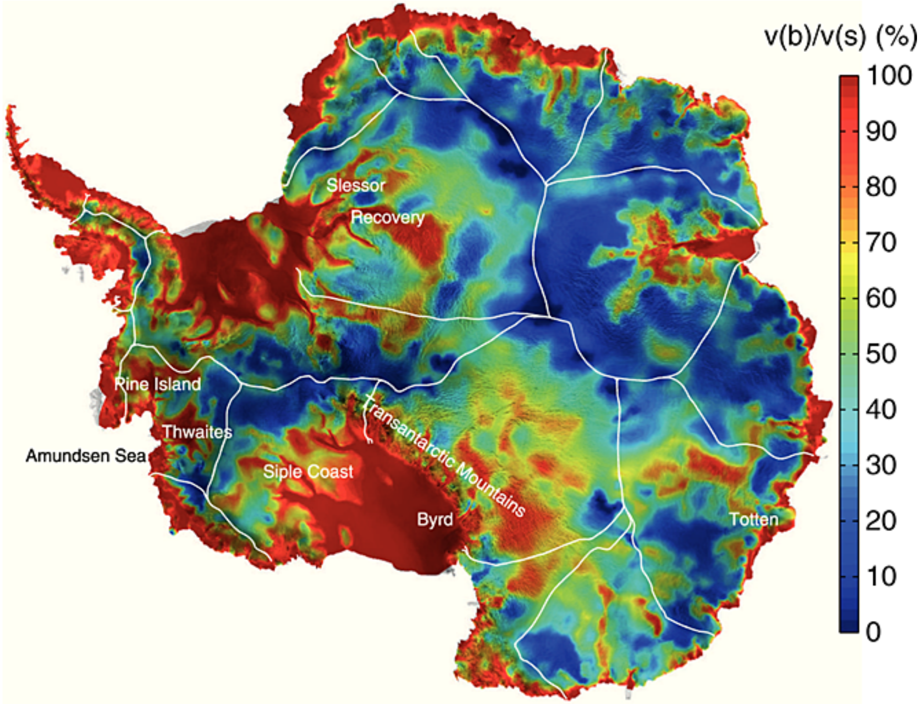

Ice sheet sectors that experience sliding tend to rest on soft sediments.

Sliding on fine grained sediments

- Why does ice slide over fine grained sediments?
- Why doesn't the ice just entrain small particles?

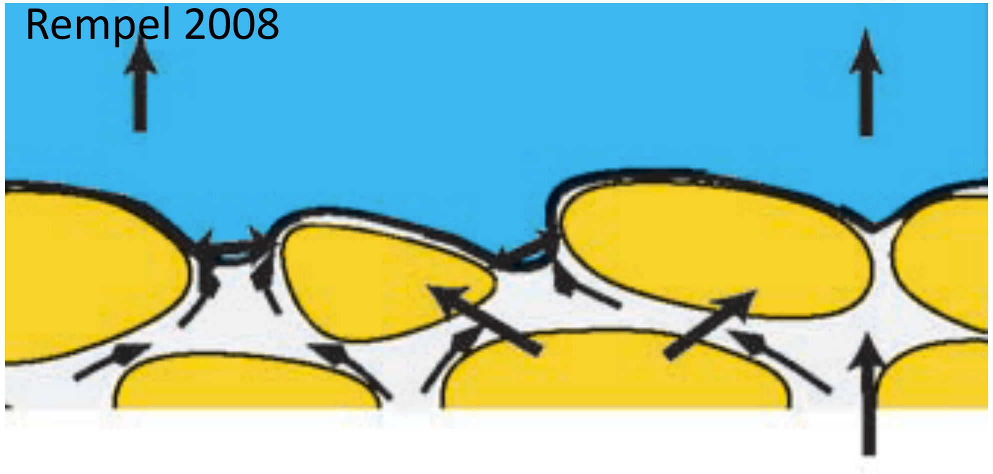

Ice Premelting: molecular thermodynamics of ice premelting

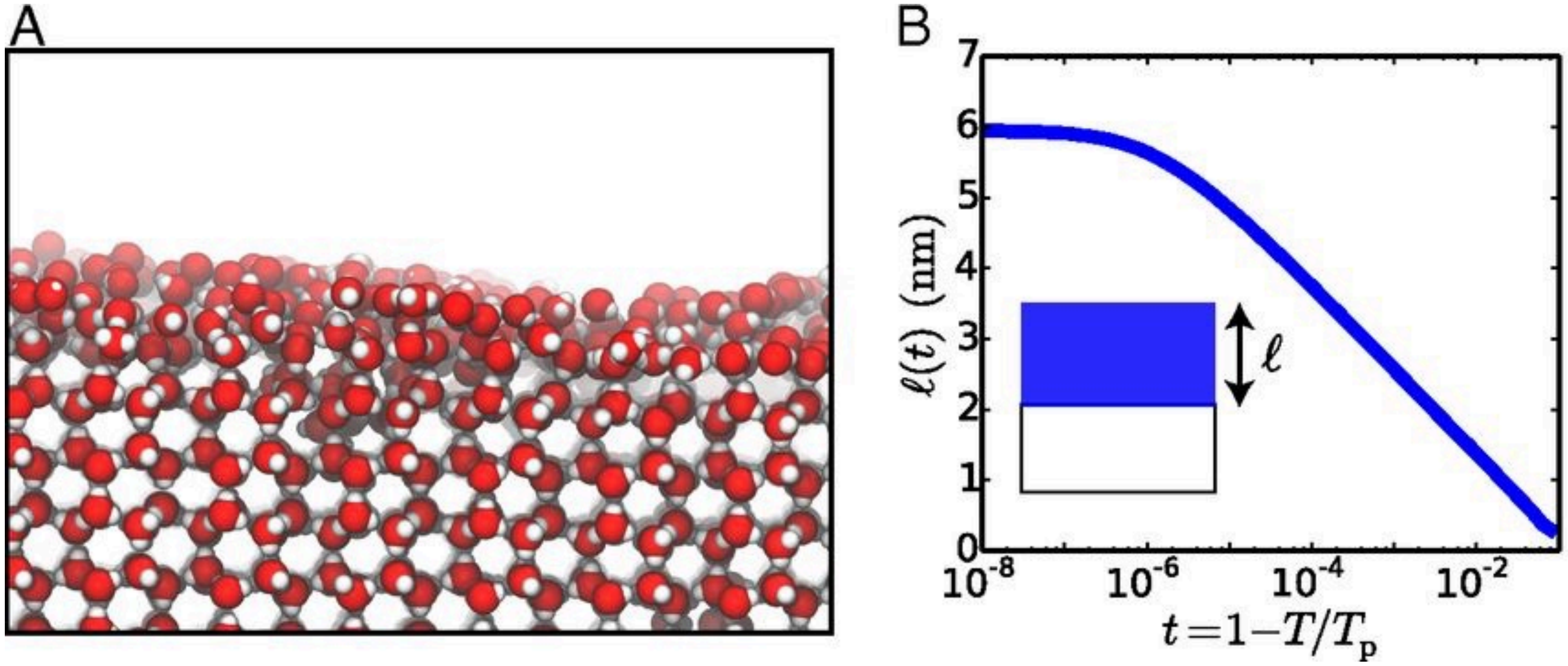

David T. Limmer PNAS 2016;113:44:12347-12349

PNAS

Ice Premelting

- Premelting occurs many (but not all) interfaces
- Premelting occurs due to the intermolecular forces that act at interfaces.
- These intermolecular forces affect many processes:
  - The transformation of snow into ice
  - The nucleation of snowflakes
  - Frost heave
  - Sediment entrainment in glacier ice
  - and glacier sliding ….

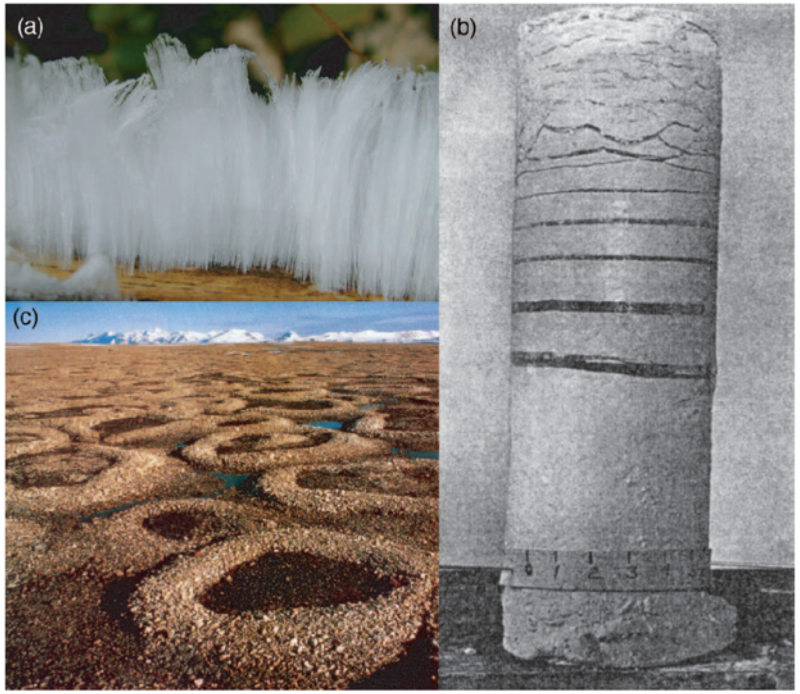

FIG. 10. (Color) Examples of frost heaving phenomena. (a) Needle ice growing out of dead wood (N. Page photo). (b) Ice lenses (dark) formed during solidification of water-saturated clay (modified from Taber, 1930, and reprinted with permission from the University of Chicago Press). (c) Stone circles in Spitspergen (B. Hallet photo, circles are 1–2 m across).

Premelting and glacier sliding

Many experiments have demonstrated that the **melting point of ice is lower**when it is contained within a porous media.

This is due to the Gibbs-Thomson effect. (Dash et al., 2007)

The more well known GT effect is that small volumes of a sustance **freeze at a lower temperature** due to surface tension…